

Beta decay of  $^{16}\text{C}$  and  $^{17}\text{N}^\dagger$ 

D. E. Alburger

Brookhaven National Laboratory, Upton, New York 11973

D. H. Wilkinson

Brookhaven National Laboratory, Upton, New York 11973

and Nuclear Physics Laboratory, Oxford, England

(Received 29 October 1975)

The delayed neutron emitters  $^{16}\text{C}$  and  $^{17}\text{N}$  have been studied with a  $^3\text{He}$  neutron detector and  $\gamma$  radiations have been measured with a Ge(Li) detector.  $^{16}\text{C}$  was formed in the reaction  $^{14}\text{C}(^{18}\text{O}, ^{16}\text{O})^{16}\text{C}$  with 56-MeV  $^{18}\text{O}$  ions, and also in the reaction  $^{11}\text{B}(^7\text{Li}, 2p)^{16}\text{C}$  with 40-MeV  $^7\text{Li}$  ions. The thermalized neutrons following both reactions yield together a  $^{16}\text{C}$  half-life of  $0.747 \pm 0.008$  sec with the well-known 4.17-sec  $^{17}\text{N}$  activity as an accompaniment formed in the  $^{14}\text{C}(^{18}\text{O}, ^{17}\text{N})^{15}\text{N}$  and  $^{11}\text{B}(^7\text{Li}, p)^{17}\text{N}$  reactions. The neutron spectra in a bare  $^3\text{He}$  detector contain  $^{16}\text{C}$  lines of  $0.79 \pm 0.03$  MeV and  $1.72 \pm 0.05$  MeV with relative intensities  $I_{0.79}/I_{1.72} = 5.4 \pm 0.7$  in addition to  $^{17}\text{N}$  peaks. The  $^{16}\text{C}$  neutron groups are assigned to the  $\beta$  decay to the known 3.36- and 4.32-MeV  $1^+$  states of  $^{16}\text{N}$  with branches of  $84.4 \pm 1.7\%$  and  $15.6 \pm 1.7\%$ , respectively. A search for  $\gamma$  rays associated with  $^{16}\text{C}$  forbidden  $\beta$  decay to the  $0^-$ ,  $3^-$ , and  $1^-$  levels of  $^{16}\text{N}$  at 0.121, 0.297, and 0.397 MeV, respectively, gave upper limits of 0.5%, 0.5%, and 0.7% for the respective branching ratios ( $\log ft > 6.85$ ,  $> 6.83$ , and  $> 6.64$ , respectively). The  $\log ft$  values for  $\beta$  decay to the 3.36- and 4.32-MeV states,  $3.551 \pm 0.012$  and  $3.83 \pm 0.05$ , respectively, compare with preliminary theoretical values of 6.49 and 3.94, respectively, due to Millener. Separate studies were made of  $^{17}\text{N}$  decay, formed in the  $^{15}\text{N}(t, p)^{17}\text{N}$  reaction at  $E_t = 3.0$  MeV. By using an empirical neutron efficiency function, established for the  $^3\text{He}$  detector with the  $^3\text{H}(p, n)^3\text{He}$  reaction,  $\beta$ -ray branches of  $^{17}\text{N}$  to the  $^{17}\text{O}$  neutron-emitting states at 4.55, 5.38, and 5.94 MeV were found to be  $39.2 \pm 2.0\%$ ,  $48.0 \pm 1.5\%$ , and  $7.9 \pm 0.3\%$ , respectively, in disagreement with two previously reported measurements.  $\gamma$ -ray measurements on  $^{17}\text{N}$  with a Ge(Li) detector yielded the following: ratio of  $\beta$ -ray branching intensities  $B_{871}/B_{3055} = 8.6 \pm 0.4$ ;  $B_{3841} < 7 \times 10^{-5}$  corresponding to  $\log ft > 8.5$  for this  $\beta$ -ray branch, thereby more firmly fixing the  $^{17}\text{N}$  spin as  $J^\pi = 1/2^-$ ; energy of  $^{17}\text{O}$  second-excited state  $3055.2 \pm 0.3$  keV; and ground-state  $\gamma$ -ray branch from the 3055.2-keV level  $< 1.5\%$ . The mirror  $\beta$  decays of the  $A = 17$  system are discussed. An incidental result is a half-life of  $178.3 \pm 0.4$  msec for  $^9\text{Li}$  formed in the  $t(^7\text{Li}, p)^9\text{Li}$  reaction with 20–40-MeV  $^7\text{Li}$  ions.

[ RADIOACTIVITY  $^{16}\text{C}$ ,  $^{17}\text{N}$ ; measured  $t_{1/2}$ ,  $E_n$ ,  $I_n$ ,  $I_\gamma$ ; deduced  $\log ft$ , decay schemes; compared with theory.  $^9\text{Li}$ ; measured  $t_{1/2}$ . ]

## I. INTRODUCTION

Our confidence that we are on the right lines in our theoretical description of nuclear structure stems largely from agreement between theory and experiment in respect of level schemes and related static and dynamical properties in cases where "complete" shell model calculations can be performed. By "complete" we mean calculations in which the valence nucleons and holes are permitted the freedom of all the relevant subshells, e.g., both  $1p_{3/2}$  and  $1p_{1/2}$  in the  $1p$  shell and  $1d_{5/2}$ ,  $2s_{1/2}$ , and  $1d_{3/2}$  in the  $2s, 1d$  shell. In the  $1p$  shell the two-body matrix elements (2BME) are sufficiently few (15) for them to be determined empirically by fitting to well-identified levels in the classic manner of Cohen and Kurath<sup>1</sup> and comparing them *ex post facto* with  $G$ -matrix elements derived from some fancied nucleon-nucleon potential. It has for many years been a source of satisfaction that these empirical 2BME generate wave functions that de-

scribe nuclear properties throughout the  $1p$  shell with good accuracy and also agree quite well with the  $G$ -matrix elements. In the  $2s, 1d$  shell the 2BME are too numerous to determine empirically in the first instance and the starting point becomes the  $G$ -matrix elements as in the extensive work of the Rochester-Oak Ridge-Michigan State school.<sup>2</sup> Such work, using exact diagonalization to determine the wave functions, is restricted at present to six particles or holes by the size of available computers but it can be extended throughout the shell with arbitrarily high accuracy by the Whitehead-Lanczos tridiagonalization technique.<sup>3</sup> The results of these computations in the  $2s, 1d$  shell are also most gratifying, especially if some small latitude of empirical trimming of the 2BME is allowed such as might reasonably represent the effects of systematic configuration mixing with higher shells. This gratifying agreement between theory and experiment was observed initially in both shells for the level schemes themselves.

However, we cannot have confidence in the wave functions that correctly describe the level schemes unless they also correctly describe other observable quantities, both diagonal and off diagonal, or at least have some good reason for not doing so. It is therefore most pleasing that the good agreement between theory and experiment extends also to static magnetic moments and to  $M1$  and Gamow-Teller transition matrix elements without any further adjustments of consequence except perhaps in securing best over-all agreement on the Gamow-Teller data where it is not the wave functions but rather the effective  $\beta$ -decay coupling constant that needs attention.<sup>4</sup> However, for the  $E2$  properties, both diagonal and off diagonal, an enhancement of the theoretical values through the familiar use of effective charges is needed; this device represents the effect of an essential deformation which is missing from the shell model calculations which are carried out in a spherical basis. When unrestricted Hartree-Fock calculations are made the deformation arises naturally, the  $E2$  moments are automatically enhanced, and the need for effective charges disappears.

This pleasing situation naturally raises the question as to whether the good agreement between theory and experiment will persist when mixed shells are involved in the description of the states in an essential way, i.e., when both valence particles in the  $2s, 1d$  shell and valence holes in the  $1p$  shell are simultaneously operative. This question is not a trivial one because such states obviously involve new, intershell, 2BME's describing the particle-hole interactions. In addition, the deformation that, as well as enhancing the  $E2$  moments, is responsible for effectively bringing certain states, nominally separated by  $\hbar\omega$ , much closer together than expected on a spherical basis, may now enter in a more essential way. There is now an extensive literature, to which we shall not refer in detail, on such particle-hole (p-h) effects, going back to the classic work of Elliott and Flowers in the  $A=16$  system.<sup>5</sup> Suffice it to say that very little work has been done, either experimentally or theoretically, on  $\beta$  decay that links such p-h states and that such transitions will constitute a crucial test of the wave functions devised to reproduce the locations of the states, just as earlier in the cases of the  $1p$ - and  $2s, 1d$  shells themselves. Note that allowed  $\beta$  transitions are more desirable than forbidden ones for such tests since their own (weak interaction) structure is simpler. The only cases studied are:

(i)  $^{11}\text{Be}$ . Here the ground state is "accidentally" of even parity making it a  $1p$ - $4h$  state. Both forbidden and allowed decays are observed<sup>6</sup>; there is no significant theoretical treatment.

(ii)  $^{14}\text{B}$ . This is a  $1p$ - $3h$  state and its allowed  $\beta$ -decay has been studied in detail both experimentally<sup>7</sup> and theoretically<sup>8</sup> with excellent agreement.

(iii)  $^{15}\text{C}$ . This is a  $1p$ - $2h$  state with one forbidden and several allowed transitions known.<sup>9</sup> There is no modern theoretical treatment.

(iv)  $^{16}\text{N}$ . This is a  $1p$ - $1h$  state with two forbidden and several allowed transitions known.<sup>10</sup> There is no modern theoretical treatment.

(v)  $^{17}\text{N}$ . This is a  $2p$ - $1h$  state with two forbidden and several allowed transitions known.<sup>11-13</sup> There is no modern theoretical treatment.

This sketchy survey reveals both that significant experimental data bearing on mixed-shell  $\beta$  decay exist and await modern theoretical treatment, and also that no experimental data exist involving nuclei in which the particle and hole shells both contain more than one particle and hole, respectively. In the present paper we extend the available material by a study of the  $\beta$  decay of  $^{16}\text{C}$  which, since it is a  $2p$ - $2h$  nucleus, represents the first available example of such a study where both particles and holes are multiple.

As will be seen, it turns out that, for practical reasons, our study of  $^{16}\text{C}$  decay cannot be separated from a correspondingly detailed study of  $^{17}\text{N}$  decay because we have no available means of making  $^{16}\text{C}$  free of  $^{17}\text{N}$ .  $^{17}\text{N}$ , as we have noted, is also a particle-hole nucleus whose study therefore fits into the present particle-hole program. There is, however, a completely different reason for our interest in  $^{17}\text{N}$ , and since existing data, particularly as to its allowed branching to neutron-unstable states of  $^{17}\text{O}$ , conflict rather severely with one another,<sup>12, 13</sup> we thought it worthwhile, from both points of view, to make a detailed study of  $^{17}\text{N}$  on its own account as well as to provide us with information to enable us to unravel the  $^{16}\text{C}$  decay scheme. This second reason for a careful study of  $^{17}\text{N}$  concerns our long-established interest in the mirror Gamow-Teller decay problem and its relevance to the possibility of second-class currents<sup>14</sup> in the weak interaction. Very briefly, if we study mirror Gamow-Teller transitions, for example, the negative electron decay of  $^{12}\text{B}$  to the ground state of  $^{12}\text{C}$  [characterized by  $(ft)^-$ ] and compare it with the mirror positive electron decay of  $^{12}\text{N}$  [characterized by  $(ft)^+$ ] then if we have perfect isobaric analog symmetry and if the hadronic weak axial current has no second-class piece we expect  $(ft)^+ = (ft)^-$ , i.e., an asymmetry in the intrinsic decay rates:  $\delta = [(ft)^+ / (ft)^-] - 1 = 0$ . A nonzero value of  $\delta$  could be due either to the existence of second-class currents of finite strength, which would be a matter of fundamental importance, or to a failure of perfect isobaric analog

symmetry, as between  $^{12}\text{B}$  and  $^{12}\text{N}$  in the present example, due to Coulomb or other charge-dependent forces, which would be trivial even if interesting. It turns out that when allowance is made for the *de facto* effects of the (Coulomb associated) binding energy differences as between the various initial,  $\beta$ -decaying, states of the mirror systems, then the significantly nonzero experimental  $\delta$ -values found for cases of even  $A$  correct essentially to zero with no residuum such as would then signal a genuine second-class current.<sup>15</sup> However, for odd- $A$  cases, such as the comparison of  $^{17}\text{N}$ - $^{17}\text{O}$   $\beta$  decay with the mirror  $^{17}\text{Ne}$ - $^{17}\text{F}$   $\beta$  decay sizeable  $\delta$  values persist even after correction for the isobaric analog asymmetry in the initial,  $\beta$ -decaying, states<sup>16</sup> (as between  $^{17}\text{N}$  and  $^{17}\text{Ne}$  in this example where the residual effect is  $\delta \approx 0.13$ <sup>17</sup>). As has been emphasized before,<sup>17</sup> this residual asymmetry may well be due to the lack of isobaric analog symmetry in the *final* states (as between  $^{17}\text{O}$  and  $^{17}\text{F}$  in the present example), since the final states are not common to the two sides of the mirror for odd  $A$ . The effect of this final-state asymmetry is even more difficult to calculate than that of the initial states where the procedures, even granted the wave functions, are by no means unambiguous. However, we should obviously expect the final-state asymmetry effect on the  $\beta$  decay to be bigger the greater the *de facto* nuclear final state asymmetry as between the two sides of the mirror. Indeed, the final state nuclear asymmetries in the odd- $A$  cases are large and either one or both of the "mirror" states are often in the nucleon continuum where tremendous differences between them can evidently arise. This brings us to the present point.

When we quote the experimental asymmetry  $\delta = 0.151 \pm 0.033$ <sup>18</sup> for  $A=17$  what is meant is that the detailed decay scheme of  $^{17}\text{Ne}$  to  $^{17}\text{F}$ , complete with all its branching ratios, is used to compute mirror final state by mirror final state the partial decay probabilities of  $^{17}\text{N}$  to  $^{17}\text{O}$  on the assumption of equality of  $ft$  values for mirror decays; addition of all relevant partial decay probabilities of  $^{17}\text{N}$  as computed then predicts the half-life of  $^{17}\text{N}$ ,  $t_{1/2}$  (predict) from that of  $^{17}\text{Ne}$  that would follow from full mirror symmetry of the weak and strong interactions; thus  $\delta = [t_{1/2}(\text{predict})/t_{1/2}(\text{exp})] - 1$ . If one transition dominates then this definition of  $\delta$  obviously refers predominantly to that transition but if, as with  $A=17$ , several transitions contribute significantly to the total decay rate, then such omnibus comparison may conceal important information that would be revealed if the  $ft$  comparison could be made partial mirror transition by partial mirror transition. In particular, in the present case, the hypothesis that the

omnibus  $\delta \approx 0.13$  is due to the final-state nuclear asymmetries would lead us to expect, on decomposing the  $^{17}\text{N}$   $\beta$  decay into its constituent parts, to find the largest  $\delta$  values associated with the partial transitions to those final states that differ most as between  $^{17}\text{O}$  and  $^{17}\text{F}$ . As is seen from Table III where our final conclusions are summarized, the  $A=17$  final states of chief concern are in their respective nucleon continua, and the biggest  $^{17}\text{O}$ - $^{17}\text{F}$  nuclear difference, as signaled by difference of nucleon width, is indeed seen for those mirror states for which  $\delta$  is most different from zero.

## II. EXPERIMENTAL PROCEDURES AND RESULTS

Although  $^{17}\text{N}$  can be formed readily in the  $^{15}\text{N}(t,p)^{17}\text{N}$  reaction with 3-MeV tritons from the 3.5-MeV Van de Graaff accelerator at Brookhaven National Laboratory, the known  $Q$  value of  $-3.0$  MeV for the  $^{14}\text{C}(t,p)^{16}\text{C}$  reaction means that its threshold is too close to the energy limit of the machine to allow an appreciable amount of  $^{16}\text{C}$  to be produced. We therefore sought alternate means of making  $^{16}\text{C}$  by using heavy ions from the tandem Van de Graaff facility. Two reactions that proved to be successful were  $^{14}\text{C}(^{18}\text{O}, ^{16}\text{O})^{16}\text{C}$  and  $^{11}\text{B}(^7\text{Li}, 2p)^{16}\text{C}$ . In the first case the target consisted of  $100 \mu\text{g}/\text{cm}^2$  of  $^{14}\text{C}$  deposited on a thick gold backing and the  $^{18}\text{O}$  beam energy was 56 MeV. For the second reaction a thick layer of 97% enriched  $^{11}\text{B}$  powder deposited on a Ta backing or alternatively a medium-thin layer of  $^{11}\text{B}$  on a Be backing was used with a  $^7\text{Li}$  beam energy of 40 MeV. Targets were mounted at the center of a 2.5-cm o.d. glass tube and a mechanical beam chopper was used for target irradiation.

Delayed neutrons from the induced activities were studied with a commercial  $^3\text{He}$  proportional counter 2.5-cm in diam  $\times$  30 cm long filled with a  $^3\text{He}$ -Ar mixture at 7 atm pressure. For the half-life measurements the detector and target were separated by  $\sim 2$  cm of paraffin and were then surrounded with a cubic structure of paraffin blocks measuring  $\sim 50$  cm on a side. A pulse-height window was set on the thermal peak in the detector output and the discriminator pulses were miscalced.

When neutron energy spectra were to be recorded all hydrogenous material was removed and the detector was placed up against the target tube. In some of the tandem experiments a 3-mm thick Pb absorber was wrapped around the target tube to suppress the very intense  $\beta$ -ray flux and the consequent pileup pulses.

Recording of the data was controlled by a timer programmer<sup>19</sup> which operated the beam chopper,

started and reset the multiscaler, or directed pulse-height spectra into various time bins in the  $\Sigma$ -7 computer.

#### Detector calibration

Because of our lack of confidence in calculations of the efficiency function of the  $^3\text{He}$  detector, particularly the corrections for the wall effect, we decided to determine the efficiency and spectral response empirically. This was done with essentially monoenergetic neutrons from the  $^3\text{H}(p,n)^3\text{He}$  reaction using a thin Ti- $^3\text{H}$  target consisting of Ti deposited to a thickness of  $0.5\text{ mg/cm}^2$  on a copper backing and then tritiated to an atomic ratio  $^3\text{H}/\text{Ti} \sim 0.15$  (the exact thickness and composition of the target are not important for our purposes). Protons of various energies between 2.0 and 3.4 MeV from the 3.5-MeV Van de Graaff bombarded the target, and the detector was positioned at  $0^\circ$  and 40 cm from the target, or at  $90^\circ$  and 19 cm from the target.

A typical response spectrum of the  $^3\text{He}$  detector at  $0^\circ$  when protons of 2.5 MeV were incident on the tritium target is shown in Fig. 1. In addition to the peak (and its low-energy wall-effect tail) due to the monoenergetic neutrons, there is a large thermal neutron peak resulting from the slowing down of neutrons in the target room and their return to the detector. Each such spectrum was fitted beyond the thermal peak with a function of the form

$$k(1 - AE)/(1 + e^{(E-E_m)/b}) + e^{-(E-E_0)/2\sigma^2},$$

where the first term fits the low-energy tail and

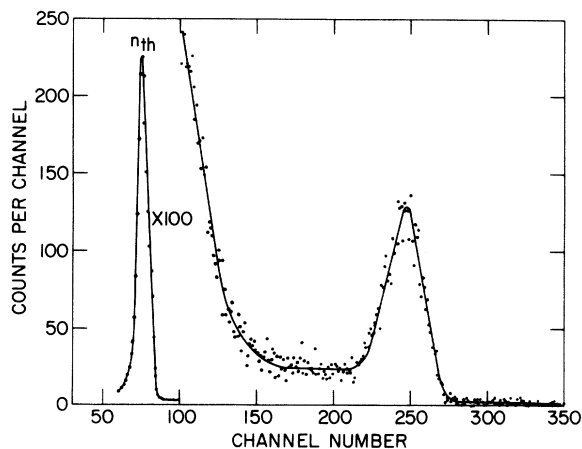


FIG. 1. Response of the  $^3\text{He}$  detector to the monoenergetic neutrons from the  $^3\text{H}(p,n)^3\text{He}$  reaction at  $E_p = 2.5\text{ MeV}$ , using a thin Ti- $^3\text{H}$  target. The large thermal neutron peak results from the slowing down of neutrons in the target room and their return to the detector.

cuts off the distribution under the peak in a physically reasonable way, and the second term is a simple Gaussian fit to the peak;  $k$ ,  $a$ ,  $b$ ,  $E_0$ , and  $\sigma$  were all computer fitted to obtain values appropriate to the final analysis of the  $^{16}\text{C}$  and  $^{17}\text{N}$  delayed neutron spectra. The effective neutron energy and total flux were calculated for the particular target-detector geometry used by numerical integration over the detector volume using the known  $^3\text{H}(p,n)^3\text{He}$  differential cross section<sup>20</sup> and the integrated beam current in each run. Small corrections were made for the scattering of neutrons in the copper target backing and glass target chamber wall. The peak efficiency was obtained by comparing the measured area under the peak with the calculated neutron flux. When this was done for all of the runs a curve of relative peak efficiency versus neutron energy was obtained. For an unknown spectrum with specified peak energies the computer program could furnish the relative intensities of the various neutron groups either by fitting the complete observed spectrum using the measured  $k(E_n)$ ,  $a(E_n)$ ,  $b(E_n)$ ,  $E_0(E_n)$ , and  $\sigma(E_n)$  or by empirically extracting the peak areas and using the peak efficiency curve.

#### Measurements on $^{16}\text{C}$ : Delayed neutrons

The decay of thermalized neutrons following a 1.5-sec bombardment of the  $^{14}\text{C}$  target with a 300 nA beam of 56-MeV  $^{18}\text{O}^{4+}$  ions is shown in Fig. 2. A channel advance rate of 0.05 sec/channel was used in the multiscaler and the data represent many irradiate-count cycles taken over a total elapsed time of  $\sim 10\text{ h}$ . Several such runs were made, as also were several using the bombardment of medium-thin targets of  $^{11}\text{B}$  with a 40-MeV  $^7\text{Li}$  beam (see below).

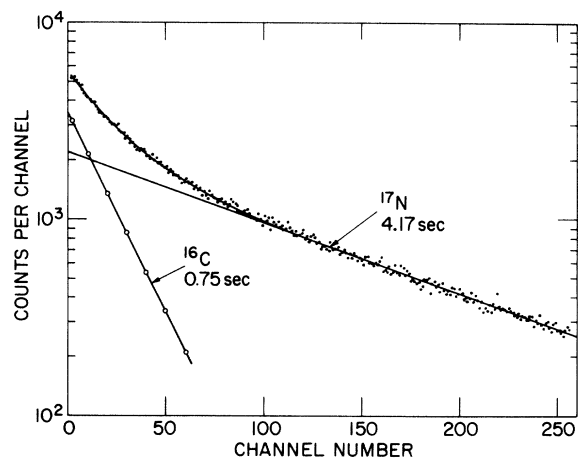


FIG. 2. The decay of thermalized neutrons following the irradiation of a  $^{14}\text{C}$  target with 56-MeV  $^{18}\text{O}$  ions.

Since  $^{17}\text{N}$  activity was obviously present in both cases, presumably made via the  $^{14}\text{C}(^{18}\text{O}, ^{17}\text{N})^{15}\text{N}$  and  $^{11}\text{B}(^7\text{Li}, p)^{17}\text{N}$  reactions, respectively, the computer fitting of the decay curve assumed two components, the unknown  $^{16}\text{C}$  and the known half-life<sup>21</sup> of  $4.169 \pm 0.008$  sec for  $^{17}\text{N}$ . The result for the half-life of  $^{16}\text{C}$  averaged from several runs was  $0.749 \pm 0.010$  sec from the first reaction and  $0.745 \pm 0.012$  sec from the second, averaging  $0.747 \pm 0.008$  sec, and in agreement with, but more accurate than, the only previous measurement<sup>22</sup> of  $0.74 \pm 0.03$  sec.

The spectrum of neutrons incident on the bare  $^3\text{He}$  detector following the  $^{18}\text{O}$  bombardment of  $^{14}\text{C}$  is shown in Fig. 3. In this run the irradiate and count intervals were 0.9 sec each, separated by 0.15 sec and the total length of the run was 32 h. Of the four peaks appearing beyond the thermal neutron peak, three can clearly be associated with  $^{17}\text{N}$  as may be seen from the  $^{17}\text{N}$  spectrum to be shown and discussed later. However, the peak at channel 260 in Fig. 3 is too intense to be due to  $^{17}\text{N}$  alone and analysis shows that about half of its intensity may be assigned to a peak of  $1.72 \pm 0.05$  MeV due to  $^{16}\text{C}$ . The other  $^{16}\text{C}$  peak at channel 160 has an energy of  $0.79 \pm 0.03$  MeV. These energies were determined by using the  $^{17}\text{N}$  peaks as an internal calibration.

In a separate test an additional delay of 2.5 sec was introduced between the irradiate and count intervals. Although this run was only 5 h in duration the statistics were sufficient to be able to show that the peak at channel 160 in Fig. 3 had virtually disappeared, while the others remained. This is consistent with the assignment of the 0.79-MeV neutron line to  $^{16}\text{C}$  decay.

Our work on  $^{16}\text{C}$  was continued by using the  $^{11}\text{B}(^7\text{Li}, 2p)^{16}\text{C}$  reaction since it was found that with a 400 nA beam of 40-MeV  $^7\text{Li}^{3+}$  ions incident on

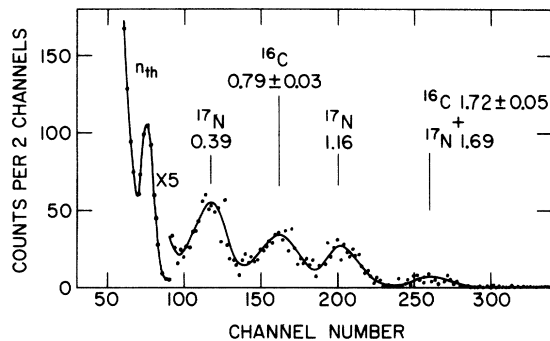


FIG. 3. The spectrum of delayed neutrons observed in a bare  $^3\text{He}$  detector following the irradiation of a  $^{14}\text{C}$  target with 56-MeV  $^{18}\text{O}$  ions. The peaks are assigned to  $^{16}\text{C}$  and  $^{17}\text{N}$  activities as discussed in the text.

the thick  $^{11}\text{B}$  target the absolute yield of  $^{16}\text{C}$  was a factor of  $\sim 20$  greater than that obtained in the  $^{14}\text{C} + ^{18}\text{O}$  reaction. A complication in this case was the production of another delayed neutron emitter 0.18-sec  $^9\text{Li}$  formed in the  $^{11}\text{B}(^7\text{Li}, ^9\text{Li})^9\text{B}$  reaction. This was apparent from the decay curve for thermalized neutrons and it was possible to extract an accurate half-life value for the  $^{16}\text{C}$  component only by waiting a time appropriate for the  $^9\text{Li}$ , of 0.18-

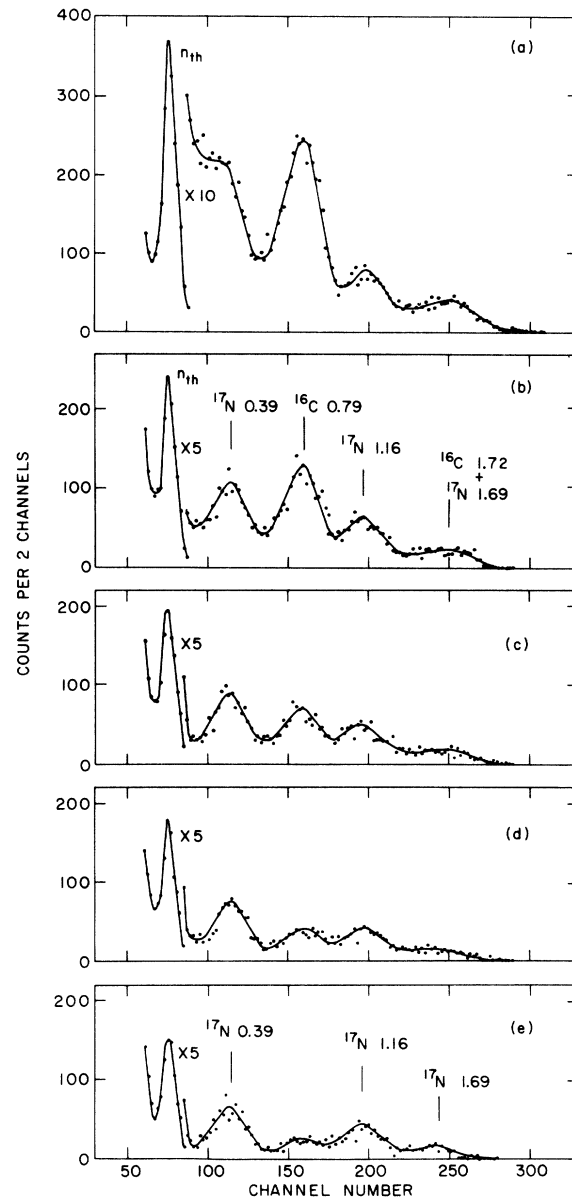


FIG. 4. The spectrum of delayed neutrons observed in a bare  $^3\text{He}$  detector following the irradiation of a thick  $^{11}\text{B}$  target with 40-MeV  $^7\text{Li}$  ions. Parts (a) through (e) are the spectra of five successive 0.75-sec time bins beginning 0.15 sec after the end of bombardment.

sec half-life, to decay to negligible proportions. This was done for the half-life measurements mentioned above. (Note that the only other known light delayed neutron emitter that we might make in our two reactions is  $^{13}\text{B}$ , which emits very few neutrons and is so short-lived—0.017 sec—that we should not see it.)

The spectrum of delayed neutrons in the bare  $^3\text{He}$  detector following the bombardment of  $^{11}\text{B}$  with 40-MeV  $^7\text{Li}$  ions was stored in five successive 0.75-sec time bins in the  $\Sigma$ -7 computer with the results shown in Fig. 4. This represents a run of 40 h using a beam current of  $\sim 150$  nA of  $^7\text{Li}^{3+}$  on the target for 1 sec in each cycle.  $^9\text{Li}$ ,  $^{16}\text{C}$ , and  $^{17}\text{N}$  all contribute to the first time bin, Fig. 4(a), but no attempt has been made to sort out the various components in this bin. Thus,  $^9\text{Li}$  is known<sup>23,24</sup> to emit neutrons with energies of  $\sim 0.3$ , 0.65, and  $\sim 1.0$  MeV. By the time of the second bin, Fig. 4(b), the  $^9\text{Li}$  activity has decayed by a factor of 18, or to nearly negligible proportions. It will be noted that the successive spectra, Figs. 4(b) through 4(e) clearly show the two  $^{16}\text{C}$  lines decaying more rapidly than the  $^{17}\text{N}$  lines. The close similarity between Fig. 3 and Fig. 4(c) may also be pointed out.

Computer fits were made to the spectra in Figs. 4(b) through 4(e) using the neutron detector efficiency functions described above together with the  $^{16}\text{C}$  and  $^{17}\text{N}$  half-lives. A portion of this analysis is given in Fig. 5 which shows the net spectrum due to the  $^{16}\text{C}$  delayed neutrons, viz., the 0.75-sec component of the four time slices used. The ratio of the neutron intensities  $I_{0.79}/I_{1.72}$  based on this spectrum is  $5.1 \pm 0.7$  in agreement with the ratio  $6.5 \pm 1.4$  derived from the  $^{14}\text{C} + ^{16}\text{O}$  data shown in Fig. 3. We adopt the value of  $5.4 \pm 0.7$  for the intensity ratio of these two  $^{16}\text{C}$  neutron groups.

The only known  $1^+$  states of  $^{16}\text{N}$ , to which  $^{16}\text{C}$  therefore enjoys allowed  $\beta$  decay, are those at  $3.355 \pm 0.005$  and  $4.318 \pm 0.005$  MeV.<sup>10</sup> Neutrons

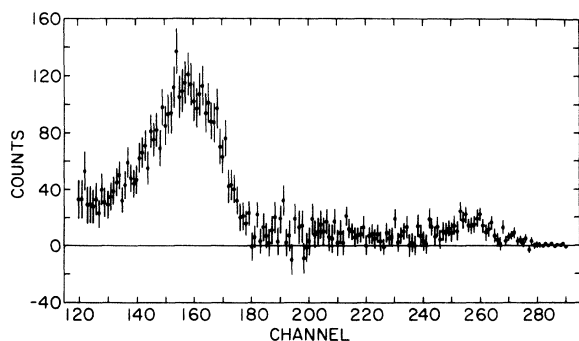


FIG. 5. Net  $^{16}\text{C}$  neutron spectrum extracted from the data of Fig. 4.

occurring in the breakup to  $^{15}\text{N}$  are expected at  $0.814 \pm 0.005$  and  $1.717 \pm 0.005$  MeV with which our measured energies of  $0.79 \pm 0.03$  and  $1.72 \pm 0.05$  MeV are in good agreement. We therefore conclude that our measurements refer to these two stated levels of  $^{16}\text{N}$ . We have no evidence for delayed neutrons such as would signal  $\beta$  decay to other states of  $^{16}\text{N}$  above the  $^{15}\text{N} + n$  threshold. In our subsequent analysis we take it that no such additional transition is significantly present. (We may anticipate the discussion by saying that we are encouraged in this neglect of possible further transitions, not only by our failure to see any, but by the theoretical prediction that no more  $1^+$  states are expected below an excitation of 6–8 MeV where their contributions to the total  $^{16}\text{C}$  decay would be negligible because of phase space even if they were intrinsically very strong.)

#### Measurements on $^{16}\text{C}$ : Delayed $\gamma$ rays

Although we have demonstrated  $^{16}\text{C}$   $\beta$  decay, as expected, to the two known  $1^+$  states of  $^{16}\text{N}$  above the  $^{15}\text{N} + n$  threshold and have no evidence for other transitions to neutron-unstable states, we cannot turn our results into  $ft$  values without knowledge of possible  $\beta$  decay to neutron-stable states of  $^{16}\text{N}$ . The only such states known<sup>10</sup> are the low-lying quartet of  $2^-$ ,  $0^-$ ,  $3^-$ , and  $1^-$  at excitation energies of zero, 0.121, 0.297, and 0.397 MeV, respectively, to all of which  $\beta$  decay is forbidden. The only transition on whose strength a useful limit can be guessed with any reliability is the unique first forbidden one to the  $2^-$  ground state. The strengths of such transitions in light nuclei do not vary very widely unless there is some evident configurational reason for their being slow which is not so in the present case. Nearby examples are the decay of this same  $2^-$  ground state of  $^{16}\text{N}$  to the ground state of  $^{16}\text{O}$  ( $\log ft = 9.11 \pm 0.04$ <sup>10</sup>) and that of  $^{17}\text{N}$  to the ground state of  $^{17}\text{O}$  ( $\log ft = 9.56 \pm 0.13$ <sup>10</sup>). In the present case the low value  $\log ft = 9.0$  would correspond to a partial half-life of more than 100 sec so we may safely ignore ground-state decay of  $^{16}\text{C}$  for our present purposes. However, we have no such reasonable guidance for the nonunique first forbidden decays to the  $0^-$  and  $1^-$  states (the third forbidden decay to the  $3^-$  state can evidently be ignored). Indeed, if the  $0^+ \rightarrow 0^-$   $\beta$  decay of  $^{16}\text{C}$  to the 0.121-MeV state of  $^{16}\text{N}$  were to have the same  $ft$  value as the  $0^- \rightarrow 0^+$   $\beta$  decay of that 0.121 MeV state to the ground state of  $^{16}\text{O}$ <sup>25</sup> it would contribute about 10% to the total  $\beta$ -decay rate of  $^{16}\text{C}$ . It is therefore important to gain information on these forbidden decays not only for their own interest but because they could possibly significantly

affect our values deduced for the strengths of the allowed decays that lead to neutron emission. This entails a search for  $\gamma$  rays from  $^{16}\text{N}$  following  $^{16}\text{C}$   $\beta$  decay.

Of the  $^{16}\text{N}$  states in question the  $0^-$  can decay only to ground with the emission of a  $\gamma$  ray of  $120.6 \pm 0.5$  keV; the  $3^-$  decays 100% to the ground state through a  $\gamma$  ray of  $297.0 \pm 0.7$  keV; the  $1^-$  decays about 27% directly to the ground state by a  $\gamma$  ray of  $397.3 \pm 0.7$  keV and the rest via the  $0^-$  state by a  $\gamma$  ray of  $276.7 \pm 0.9$  keV. We must therefore search for  $\gamma$  rays of approximately 121, 277, 297, and 397 keV, although we certainly do not expect to find the third of these.

Although the delayed neutron spectra, using both the reactions we have described, are quite clean, since delayed neutron emitters are rare, the same is not true of the  $\gamma$  spectra, since all sorts of contaminant activities are produced. It is not a wholly trivial matter even to observe the well-known ( $\approx 3\%$ ) branch of  $^{17}\text{N}$  via the  $870.81 \pm 0.22$ -keV state of  $^{17}\text{O}$ .<sup>10</sup> It is very desirable that we should indeed see this line following  $^{17}\text{N}$  decay since then, if we know the relative  $^{16}\text{C}$  and  $^{17}\text{N}$  total activities within our counting interval, we can infer the  $^{16}\text{C}$   $\gamma$ -producing branches from the known  $^{17}\text{N}$   $\gamma$ -producing branch.

We found the cleanest conditions using a few mg/cm<sup>2</sup> thick deposit on  $^{11}\text{B}$  on a 0.0025-cm thick Be foil, 40-MeV  $^7\text{Li}$  bombardment, and fast pneumatic rabbit transport to a shielded counting area. The target was viewed with a 70-cm<sup>3</sup> Ge(Li) counter of good resolution and, simultaneously, by a  $^3\text{He}$  counter immersed in a rigid paraffin assembly in such a manner as to give it an approximately constant sensitivity to neutrons across the energy range of interest from both  $^{16}\text{C}$  and  $^{17}\text{N}$  decay. By a time-decomposition into  $^{16}\text{C}$  and  $^{17}\text{N}$  lifetimes following multiscaling of the pulses due to thermalized neutrons we could determine the relative  $^{16}\text{C}$  and  $^{17}\text{N}$  production rates in the conditions of our bombardment (2:1 in favor of  $^{16}\text{C}$ ). With this information we could then calculate the relative  $^{16}\text{C}/^{17}\text{N}$  activity in any other timing regime. We used several different timing regimes depending on whether our objective was to optimize sensitivity to  $^{16}\text{C}$  decay,  $^{17}\text{N}$  decay and so on.

The 871-keV line following the decay of  $^{17}\text{N}$  made in the  $^{11}\text{B} + ^7\text{Li}$  bombardment was weak and in a region of high background. However, it was clearly identified by the following tests:

(i) *Energy*. We found a line of  $870.95 \pm 0.22$  keV which is to be compared with the expected  $870.79 \pm 0.22$  keV.

(ii) *Lifetime*. Our 871-keV line decayed with a half-life of  $4.5 \pm 0.8$  sec to be compared with the expected 4.17 sec.

TABLE I.  $\beta$  decay of  $^{16}\text{C}$ .

Final state in $^{16}\text{N}$ (MeV)	$J^\pi$	$\beta$ branch <sup>a</sup> (%)	$\log ft$ (exp)	$\log ft$ <sup>b</sup> (theor)
0.121	$0^-$	<0.5	>6.85	...
0.297	$3^-$	<0.5	>6.83	...
0.397	$1^-$	<0.7	>6.64	...
3.36	$1^+$	$84.4 \pm 1.7$	$3.551 \pm 0.012$	6.49
4.32	$1^+$	$15.6 \pm 1.7$	$3.83 \pm 0.05$	3.94

<sup>a</sup> Note that the limits on the  $\beta$  branches to the three odd-parity states are linked since the most sensitive index of the formation of the  $1^-$  state is its branch ( $\approx 70\%$ ) via the  $0^-$  state; because of this the limit on the combined  $\beta$  branching to these three low-lying states is 1.2%.

<sup>b</sup> Reference 28.

(iii) *Intensity*. In clean conditions on the 3.5 MeV Van de Graaff accelerator we made  $^{17}\text{N}$  via the reaction  $^{15}\text{N}(t,p)^{17}\text{N}$  and viewed the target with the same  $^3\text{He}$ -counter/paraffin assembly and the same Ge(Li) counter as in the  $^{11}\text{B} + ^7\text{Li}$  experiment and in a similar geometry in relation to the target. The 871-keV line was now very easily seen and we measured its peak counts per neutron count in the  $^3\text{He}$  counter. In the  $^{11}\text{B} + ^7\text{Li}$  run the 871-keV peak stood in relation to those counts in the  $^3\text{He}$  counter that belonged to  $^{17}\text{N}$  in a proper way as determined from this  $^{15}\text{N} + t$  experiment.

The  $^{16}\text{N}$  lines were sought under optimum conditions in which the 871-keV line from  $^{17}\text{O}$  was clearly visible and of well-determined strength. The search was carried out using a computer program in which the Ge(Li) resolution was fixed at measured values as determined from neighboring  $\gamma$ -ray lines and at small energy intervals covering ranges 2 keV either side of the nominal  $\gamma$ -ray energies. No  $^{16}\text{N}$  line was found and limits on the associated  $^{16}\text{C}$   $\beta$  branches were extracted as shown in Table I using the methods already detailed, (3.3  $\pm$  0.5)% for the yield of the 871-keV line per  $^{17}\text{N}$  decay,<sup>11,12</sup> and a peak-efficiency calibration of the Ge(Li) detector carried out using a set of standard sources of known intensities with the same  $\beta$  absorber in place in front of the Ge(Li) detector as in the  $^{11}\text{B} + ^7\text{Li}$  run.

We ignore the possible forbidden branches in prescribing the data on the allowed transitions in Table I.

#### Measurements on $^{17}\text{N}$ : Delayed neutrons

$^{17}\text{N}$  was produced in the  $^{15}\text{N}(t,p)^{17}\text{N}$  reaction by bombarding a Ti<sup>15</sup>N target with 3.0-MeV tritons from the 3.5-MeV Van de Graaff. Following an irradiation of 4 sec duration the spectrum was

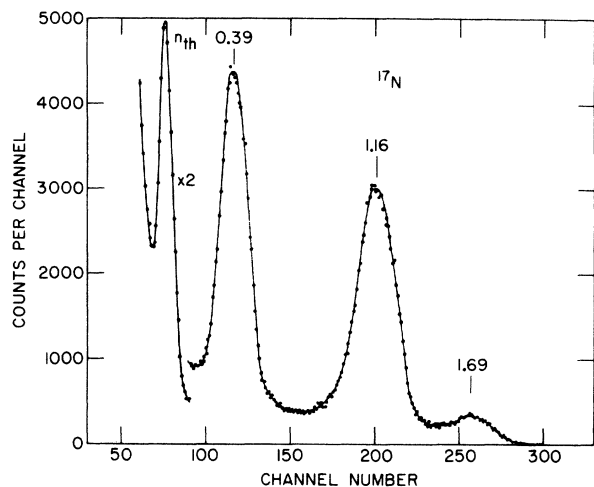


FIG. 6. The spectrum of delayed neutrons observed in a  $^3\text{He}$  detector due to  $^{17}\text{N}$  activity formed in the  $^{15}\text{N}(t, p)^{17}\text{N}$  reaction at  $E_t = 3.0$  MeV.

stored for 4 sec, this cycle being controlled by the timer programmer and repeated until sufficient numbers of counts were accumulated.

Figure 6 shows one of the  $^{17}\text{N}$  spectra obtained with the  $^3\text{He}$  detector close to the glass target tube. An analysis of this spectrum was made using the techniques referred to earlier. The results are shown in Table II, which also includes the branching ratios obtained in two previously reported measurements.<sup>12,13</sup> In reducing our own data we have taken as the sum of the  $\beta$  branches to neutron-stable levels of  $^{17}\text{O}$  ( $4.9 \pm 0.7\%$ ), being a conflation of earlier measurements.<sup>11, 12</sup>

As described earlier, the  $^3\text{He}$  detector response for neutrons of various energies was taken in relatively good geometry. Since it was thought that the response function might depend on the source-

detector distance, another run was made on the  $^{17}\text{N}$  neutron spectrum with the detector at a distance of 27 cm from the target. Analysis of the relative peak intensities in this run showed no discernible differences with the data from Fig. 6.

#### Measurements on $^{17}\text{N}$ : $\gamma$ -ray spectrum

The  $\gamma$ -ray spectrum of  $^{17}\text{N}$  was studied using a Ge(Li) detector together with a rabbit target-transfer system at the 3.5-MeV Van de Graaff. A target of  $\text{Ti}^{15}\text{N}$  was attached to a rabbit and bombarded with 3.0-MeV tritons. The activity was monitored by observing thermalized neutrons with a  $^3\text{He}$  counter surrounded with paraffin and placed opposite to the Ge(Li) detector. The paraffin also provided an energy calibration line of  $2223.31 \pm 0.04$  keV from  $n-p$  capture of the  $^{17}\text{N}$  neutrons. This line, together with the  $2103.58 \pm 0.10$ -keV one-escape peak due to the 2614.58-keV  $\gamma$  ray of a  $^{228}\text{Th}$  source, allowed the higher energy  $^{17}\text{N}$   $\gamma$  ray to be measured as  $2184.2 \pm 0.2$  keV. By adding the recoil energy correction of 0.16 keV and the energy of the first excited state,  $870.8 \pm 0.2$  keV,<sup>10</sup> the energy of the  $^{17}\text{O}$  second excited state becomes  $3055.2 \pm 0.3$  keV, to be compared with the compilation value<sup>10</sup> of  $3055 \pm 2.5$  keV.

In this same run the relative intensities of the 870.8- and 2184.2-keV peaks were found, as well as upper limits on 3055- and 3841-keV lines neither of which could be seen in the spectrum. A separate run was made using a  $^{56}\text{Co}$  source to establish the  $\gamma$ -ray efficiency versus energy function for the detector. Tables of Camp and Meredith<sup>26</sup> were used for the relative intensities of the  $^{56}\text{Co}$   $\gamma$  rays. By applying this efficiency function to the  $^{17}\text{N}$   $\gamma$ -ray peaks we find  $I_{871}/I_{2184} = 9.6 \pm 0.4$ . This ratio is considerably larger than the earlier reported ratios of  $6.8 \pm 0.9$ <sup>11</sup> and  $6.36 \pm 0.20$ <sup>12</sup> both

TABLE II.  $\beta$  ray branches in the decay of  $^{17}\text{N}$ .

State in $^{17}\text{O}$ (MeV)	$\beta$ -ray branch (%)			$\log ft^a$
	Previous		Present	
0	$1.6 \pm 0.5^b$		...	$7.29 \pm 0.11$
0.871	$2.8 \pm 0.5^c$		$3.0 \pm 0.5$	$6.80 \pm 0.07$
3.055	$0.50 \pm 0.10^c$		$0.34 \pm 0.06$	$7.08 \pm 0.08$
3.841	$<0.1^b$		$<7 \times 10^{-3}$	$>8.5$
4.554	$37.9 \pm 1.8^d$	$27 \pm 3^e$	$39.2 \pm 2.0$	$4.40 \pm 0.02$
5.377	$51.1 \pm 1.5^d$	$57 \pm 4^e$	$48.0 \pm 1.5$	$3.88 \pm 0.02$
5.935	$5.8 \pm 0.6^d$	$11 \pm 2^e$	$7.9 \pm 0.7$	$4.31 \pm 0.04$

<sup>a</sup> Based on present results, except for the ground-state branch.

<sup>b</sup> Reference 11.

<sup>c</sup> Combined result based on Refs. 11, 12, and 13.

<sup>d</sup> Reference 12.

<sup>e</sup> Reference 13.



of which were obtained using NaI(Tl) detectors. A possible explanation might be incomplete exclusion of the  $np \rightarrow d\gamma$  radiation of 2.22 MeV in the earlier work; this would interfere with the 2.18-MeV peak in the NaI(Tl) spectrum whereas it is completely resolved in our own case. Assuming that 3.3% of the  $^{17}\text{N}$  decays result in 870.8-keV  $\gamma$  rays then the upper limit on the intensity of a 3841-keV  $\gamma$  ray is  $< 7 \times 10^{-5}$  per decay (90% confidence limit) corresponding to  $\log ft > 8.5$  for  $\beta$  decay to the  $J^\pi = \frac{5}{2}^-$  3841-keV state. This is an improvement by a factor of more than 10 on the old limit<sup>11</sup> and correspondingly reinforces the assignment of  $J = \frac{1}{2}$  to  $^{17}\text{N}$ . From the limit on the 3055-keV line the ground-state  $\gamma$ -ray branch from the 3055-keV level is  $< 1.5\%$ ; a very small branch would be expected in view of its being an  $M2$  in competition with the 2184-keV  $E1$  to the first-excited state.

#### Half-life of $^9\text{Li}$

As in the case of  $^{16}\text{C}$  the threshold for the  $^7\text{Li}(t, p)^9\text{Li}$  reaction is too high for  $^9\text{Li}$  to be made with the 3.5-MeV Van de Graaff. We therefore studied this activity by using the inverse reaction, i.e.,  $^3\text{H}(^7\text{Li}, p)^9\text{Li}$  at  $^7\text{Li}$  beam energies in the range 20–40 MeV from the MP tandem Van de Graaff facility. It was hoped that the neutron spectrum in the  $^3\text{He}$  detector could be measured so that independent evidence could be obtained on the characteristics of the decay of  $^9\text{Li}$ . Two previous studies<sup>23, 24</sup> of  $^9\text{Li}$  have been made, both using the  $\beta$ -neutron time-of-flight technique, but substantial differences in the  $\beta$  branching ratios were found in these experiments.

A Ti- $^3\text{H}$  target with a 2.5-mg/cm<sup>2</sup> deposit of Ticon a copper backing tritiated to an atomic ratio  $^3\text{H}/\text{Ti} = 0.85$  was mounted in a glass target chamber. In order to protect the tandem accelerator vacuum system from possible tritium contamination the

target tube and a short intermediate beam pipe section were isolated from the main beam pipe by means of a 0.00025-cm thick Ni foil. The target section was filled with He gas at low pressure ( $\sim 2$  cm Hg) and a fast-acting shutoff valve was located on the high-vacuum side of the foil, together with an ionization gauge to detect any leakage of gas through the foil.  $^7\text{Li}^{3+}$  beam currents of  $\sim 500$  nA were used but no foil rupture occurred.

Unfortunately, the yield of delayed neutrons in the bare  $^3\text{He}$  detector from  $^9\text{Li}$  produced with the most intense  $^7\text{Li}$  beams available was much too small to define the shape of the spectrum in a reasonable amount of machine time. However, with paraffin surrounding the target and detector there was enough yield of thermalized neutrons to allow the half-life to be determined. In addition to the  $^9\text{Li}$  neutrons there was a background of 4.17-sec  $^{17}\text{N}$  presumably produced via the  $^{12}\text{C}(^7\text{Li}, 2p)^{17}\text{N}$  reaction on carbon contamination. This yield was  $\sim 1\%$  as strong as the  $^9\text{Li}$  at the beginning of each measurement.

Eleven runs were made on the  $^9\text{Li}$  half-life using various beam energies and intensities. The computer fits to the data assumed two components, the  $^9\text{Li}$  unknown and the 4.169-sec background due to  $^{17}\text{N}$ . Based on the analysis of the various runs a half-life value of  $178.3 \pm 0.4$  msec is adopted for  $^9\text{Li}$ . The result agrees with a previous value of  $177 \pm 3$  msec obtained by Chen, Tombrello, and Kavanagh<sup>24</sup> but differs by more than the sum of errors when compared with the previous most accurate value of  $176 \pm 1$  msec reported by Dostrovsky *et al.*<sup>27</sup>

#### III. DISCUSSION: $^{16}\text{C}$

Our experimental conclusions as to  $^{16}\text{C}$  decay are summarized in Fig. 7 and in Table I, the latter also showing Millener's preliminary theoretical  $ft$  values for the two allowed transitions.<sup>28</sup> It is clear that theory and experiment disagree rather badly both in respect of the relative  $ft$  values of these two transitions, where we have  $[(ft)_{4.32}/(ft)_{3.36}]_{\text{exp}} = 1.89 \pm 0.22$  as against  $[(ft)_{4.32}/(ft)_{3.36}]_{\text{theor}} = 0.003$ , and also in respect to the total decay rates where we have  $t_{1/2}(\text{exp}) = 0.747 \pm 0.008$  sec as against  $t_{1/2}(\text{theor}) = 6.2$  sec.

Millener's theoretical  $ft$  values follow from a detailed calculation using particle-hole 2BME's that proved highly successful in the case of  $^{14}\text{B}$ .<sup>8</sup> Failure in the present case is perhaps the more surprising since weak  $\beta$  transitions to the two low-lying  $1^+$  states of  $^{16}\text{N}$  are theoretically predicted, on the basis of a simple weak-coupling argument<sup>28</sup> such as we should have expected, to

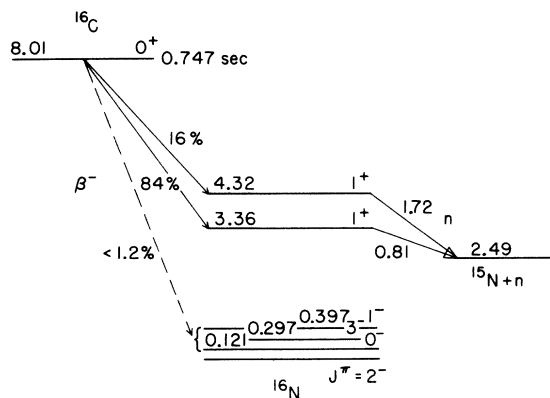


FIG. 7. Proposed decay scheme of  $^{16}\text{C}$  based on the present work.

give at least a reasonable qualitative indication of how things might turn out. On this weak-coupling argument the  $^{16}\text{C}$  ground state is chiefly  $(^{14}\text{C } 0_1^+)(^{18}\text{O } 0_1^+)$  with some  $(^{14}\text{C } 0_1^+)(^{18}\text{O } 0_2^+)$  expected; detailed evaluation gives about 67%  $L=0$  and 32%  $L=1$ . Similarly, the lowest weak coupling basis states for  $1^+$  in  $^{16}\text{N}$  are  $(^{14}\text{N } 1_1^+)(^{18}\text{O } 0_1^+)$  and then  $(^{14}\text{C } 0_1^+)(^{18}\text{F } 1_1^+)$ . Now  $(^{14}\text{N } 1_1^+)(^{18}\text{O } 0_1^+)$  are predominantly  $L=2$  and 0, respectively, so weak  $\beta$  decay is expected to the lower of the  $^{16}\text{N } 1^+$  states. The second  $1^+$  state is mainly of  $L=0$  but the symmetry is chiefly [4431], whereas the dominant symmetry of the  $^{16}\text{C}$  ground state is [4422] and the  $\beta$  decay is again expected to be weak. It is therefore even qualitatively surprising that both  $^{16}\text{C}$   $\beta$  branches that we observed are strong rather than weak.

The detailed theoretical treatment<sup>28</sup> indeed predicts that  $^{16}\text{N}$  should have three  $1^+$  states to which  $^{16}\text{C}$   $\beta$  decay is strong, with  $\log ft$  values in the range 3.2 to 3.8, but these theoretical states are at much higher excitation (about 6–8 MeV). Obviously the two low-lying  $1^+$  states will be sensitive to mixing with each other on changes of the 2BME and so this failure of theory to get the relative  $ft$  values right might be remedied without too much difficulty. Indeed, if we arbitrarily mix the two theoretical low-lying  $1^+$  wave functions  $\psi_1$  and  $\psi_2$  to construct new states,  $\psi_1' = 0.6\psi_1 + 0.8\psi_2$  and  $\psi_2' = 0.8\psi_1 - 0.6\psi_2$ , the ratio of the  $ft$  values comes about right and the theoretical  $^{16}\text{C}$  half-life simultaneously shortens from 6.2 sec to 2.7 sec which is much nearer the experimental 0.75 sec, if still not good.

It is not therefore clear whether or not some unexpectedly significant revision in the making of these mixed-shell calculations may be necessary. This would be surprising in view of the success of the particle-hole interaction, used in the present calculation, in correlating the properties of the low-lying "wrong parity" states in the  $1p$  shell,<sup>8</sup> in particular the relative lowering of the  $2s$  relative to the  $1d$  states as one moves to smaller  $A$  values. It would also be surprising in view of the fact that the particle-hole interaction used is quite close to the Kuo  $G$  matrix derived from a realistic nucleon-nucleon potential. A final remark is that although the calculation may have failed quite badly on the  $ft$  values it gives good agreement with experiment on the  $^{16}\text{N}$  level scheme itself<sup>28</sup> which emphasizes the point made in the Introduction that an account of the level scheme alone is not enough.

It should be emphasized that Millener's theoretical results are preliminary and may possibly change significantly with refinement even without much change to the particle-hole interaction used.

In particular, in the  $\text{SU}(3)$  basis used for the detailed calculation only those representations free of spurious center-of-mass effects are admitted at present (a restriction that can be lifted in principle) and this truncation might possibly adversely affect the  $ft$  values without adversely affecting the level scheme of  $^{16}\text{N}$  (which in fact looks good in terms of relative excitation within itself but which lies about 2 MeV too high as a whole relative to  $^{16}\text{C}$  and which will be pushed down somewhat by an expansion of the  $\text{SU}(3)$  basis).

#### IV. DISCUSSION: $^{17}\text{N}$

As is seen from Table II, there are serious discrepancies among the three recent measurements of the  $^{17}\text{N}$   $\beta$  branches to the neutron-unstable states of  $^{17}\text{O}$ . In the subsequent analysis we shall therefore use just our own numbers for those branches; for the branches to the neutron-stable excited states we combine our new results with the means of values earlier obtained.<sup>11-13</sup> The  $^{17}\text{N}$  decay scheme is shown in Fig. 8.

From the point of view of nuclear structure theory the present data affect the previous discussion<sup>12</sup> only marginally and since there has been no significant new theoretical discussion, although new developments are under way,<sup>28</sup> we will leave this matter merely with the reminder that theory and experiment do not, at the moment, sit at all well together.

Our chief present concern is with the mirror  $ft$ -value problem which is summarized in Table III

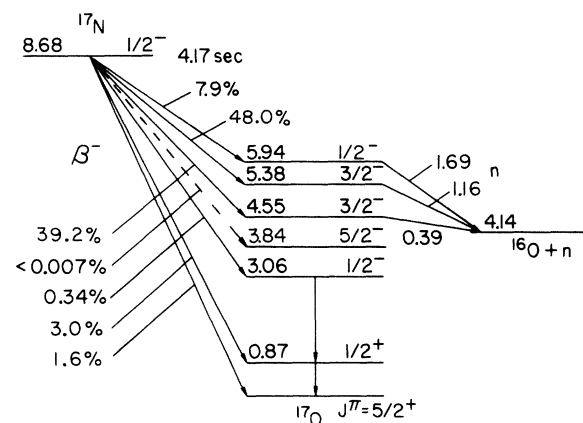


FIG. 8. Decay scheme of  $^{17}\text{N}$ . The  $\beta$ -ray branch to the ground state of  $^{17}\text{O}$  state is from Ref. 11, while the branches to the first two excited states were derived by combining the present results with those of Refs. 11, 12, and 13.  $\beta$ -ray branches to the three neutron-emitting states of  $^{17}\text{O}$ , and the limit on the branch to the 3.84-MeV state, are from the present work only.

TABLE III. Summary of  $^{17}\text{N}$  and  $^{17}\text{Ne}$   $\beta$  decay relevant to the mirror Gamow-Teller  $ft$  value problem. The underlying data are detailed in the text.  $\Gamma_n$  and  $\Gamma_p$  are the neutron and proton widths of the  $^{17}\text{O}$  and  $^{17}\text{F}$  states, respectively (Ref. 10).  $(ft)^-$  is for  $^{17}\text{N}$  decay and  $(ft)^+$  for  $^{17}\text{Ne}$  decay.

Final state in $^{17}\text{O}$ (MeV)	Final state in $^{17}\text{F}$ (MeV)	$J^\pi$	$\Gamma_n$ (keV)	$\Gamma_p$ (keV)	$(ft)^-$	$(ft)^+$	$\delta$
3.055	3.105	$\frac{1}{2}^-$	0	19	$(8.0 \pm 1.1) \times 10^6$	$(2.78 \pm 0.40) \times 10^6$	$-0.653 \pm 0.069$
4.554	4.605	$\frac{3}{2}^-$	40	230	$(2.53 \pm 0.14) \times 10^4$	$(3.92 \pm 0.18) \times 10^4$	$0.55 \pm 0.11$
5.377	5.477	$\frac{3}{2}^-$	28	69	$(7.59 \pm 0.28) \times 10^3$	$(7.22 \pm 0.15) \times 10^3$	$-0.049 \pm 0.040$
5.935	6.041	$\frac{1}{2}^-$	23	28	$(2.04 \pm 0.19) \times 10^4$	$(2.606 \pm 0.067) \times 10^4$	$0.28 \pm 0.12$

where the relevant data are assembled. For the ground state transition energies we have used the new mass tables,<sup>29</sup> in the case of the mass of  $^{17}\text{Ne}$  combining the value from the tables with the result of the application of the isobaric multiplet mass equation to the other members of the  $T = \frac{3}{2}$  isobaric quartet.<sup>18</sup> For the excitation energies in  $^{17}\text{O}$  we have followed the compilation<sup>10</sup> and for those in  $^{17}\text{F}$  we have used the means of the two concordant sets quoted in Ref. 30 from which we also take the  $^{17}\text{Ne}$  branching ratios and half-life. The  $^{17}\text{N}$  half-life is our own.<sup>18</sup>

Comparison of Tables II and III shows that the omnibus  $\delta \approx 0.15$  is due chiefly to the very large positive  $\delta$  value for the lower  $\frac{3}{2}^-$  state to which the  $^{17}\text{N}$  branch is about 39% (the comparably negative  $\delta$  value for the lower  $\frac{1}{2}^-$  state is unimportant in the omnibus  $\delta$  because the branching ratio of  $^{17}\text{N}$  to that state is only about 0.3%).

These enormous  $\delta$  values for the two lowest states, by far more different from zero than any case observed in the even- $A$  systems where the final state is common to the two sides of the mirror, reveal very clearly the importance of the final state nuclear asymmetry in the odd- $A$  cases and confirm the reasonableness of excluding these cases from the analyses of  $ft$ -asymmetries in terms of second-class currents.<sup>15</sup> It is particularly noteworthy that the largest  $\delta$  values are found in the two cases where the nuclear asymmetry is most evident: for the lower  $\frac{1}{2}^-$  state  $^{17}\text{O}$  is neutron stable while its mirror is in the continuum; for the lower  $\frac{3}{2}^-$  state the difference between the two nuclear widths is very large. (In the former case the large  $ft$  value in any case makes a large "accidental"  $\delta$  value more likely.<sup>31</sup>)

It is worth making some remarks on the other two cases of odd- $A$  systems that have large residual  $\delta$  values after allowance for the nuclear

asymmetry in the initial state, namely  $A = 9$  and  $25$ <sup>17</sup> ( $A = 13$  at one time appeared to be another such case<sup>17</sup> but a treatment of the initial state nuclear asymmetry using more modern wave functions has shown that it can account for the experimental  $\delta$  value<sup>32</sup>).  $A = 9$  is a very similar case to  $A = 17$  in that continuum final states are involved: the decay of  $^9\text{Li}$  is about two-thirds to the ground state of  $^9\text{Be}$  which is neutron stable, whereas its mirror in  $^9\text{B}$  that receives the  $^9\text{C}$  positron decay is in the proton continuum; most of the rest of  $^9\text{Li}$   $\beta$  decay leads to the 2.43 MeV  $\frac{5}{2}^-$  level of neutron width only 1 keV, whereas the mirror level in  $^9\text{B}$  has a proton width of 80 keV,<sup>10</sup> so a gross nuclear asymmetry is evident in both cases and an aberrant  $\delta$  value may well be anticipated in consequence.  $A = 25$  does not involve continuum levels significantly, although the continuum is close for the major  $\beta$  branches of  $^{25}\text{Na}$ ; in this case the experimental error on  $\delta$  is quite large, and full many-particle wave functions have not been available to assess the initial state binding energy effect so judgement must be reserved. (It is interesting to note that for  $A = 13$  the bulk of the  $\beta$  decay leads to nucleon-stable states in  $^{13}\text{C}$  and  $^{13}\text{N}$  so we should not expect there as large a final-state nuclear asymmetry effect as for  $A = 9$  and  $A = 17$ ; it is therefore pleasing that the initial state effect now appears adequate to explain the experimental  $\delta$  value.<sup>32</sup>)

#### ACKNOWLEDGMENTS

We are very grateful to Dr. D. J. Millener for discussions of the  $^{16}\text{C}$  problem and for allowing us to quote from his unpublished work. We are also indebted to Dr. Keith Jones for helpful suggestions and for assistance in several of the experiments.

- †Research at Brookhaven National Laboratory carried out under the auspices of the U.S. Energy Research and Development Administration. Work at Oxford University supported by a Royal Society Grant in Aid.
- <sup>1</sup>S. Cohen and D. Kurath, *Nucl. Phys.* 73, 1 (1965); see also D. Amit and A. Katz, *Nucl. Phys.* 58, 388 (1964).
- <sup>2</sup>J. B. French, E. C. Halbert, J. B. McGrory, and S. S. M. Wong, *Adv. Nucl. Phys.* 3, 193 (1969); E. C. Halbert, J. B. McGrory, B. H. Wildenthal, and S. P. Pandya, *ibid.* 4, 316 (1971).
- <sup>3</sup>See, e.g., B. J. Cole, A. Watt, and R. R. Whitehead, *J. Phys.* A7, 1399 (1974).
- <sup>4</sup>D. H. Wilkinson, *Nucl. Phys.* A209, 470 (1973).
- <sup>5</sup>J. P. Elliott and B. H. Flowers, *Proc. Roy. Soc. (London)* A242, 57 (1957).
- <sup>6</sup>D. E. Alburger and D. H. Wilkinson, *Phys. Rev. C* 3, 1492 (1971).
- <sup>7</sup>D. E. Alburger and D. R. Goosman, *Phys. Rev. C* 10, 912 (1974).
- <sup>8</sup>D. J. Millener and D. Kurath, Oxford Nuclear Physics Laboratory Report No. 40/75 (unpublished).
- <sup>9</sup>D. E. Alburger and K. W. Jones, *Phys. Rev.* 149, 743 (1966).
- <sup>10</sup>F. Ajzenberg-Selove, *Nucl. Phys.* A166, 1 (1971).
- <sup>11</sup>M. G. Silbert and J. C. Hopkins, *Phys. Rev.* 134, B16 (1964).
- <sup>12</sup>A. R. Poletti and J. G. Pronko, *Phys. Rev. C* 8, 1285 (1973).
- <sup>13</sup>R. J. de Meijer, C. Delaune, D. McShan, J. W. Nelson, and H. A. van Rinsvelt, *Nucl. Phys.* A209, 424 (1973).
- <sup>14</sup>S. Weinberg, *Phys. Rev.* 112, 1375 (1958).
- <sup>15</sup>D. H. Wilkinson, *Phys. Lett.* 48B, 169 (1974).
- <sup>16</sup>D. H. Wilkinson, *Phys. Rev. Lett.* 27, 1018 (1971).
- <sup>17</sup>D. H. Wilkinson, in *Few Particle Problems in the Nuclear Interaction* (North-Holland, Amsterdam, 1972), p. 191.
- <sup>18</sup>D. E. Alburger and D. H. Wilkinson, *Phys. Rev. C* 6, 2019 (1972).
- <sup>19</sup>G. E. Schwender, D. R. Goosman, and K. W. Jones, *Rev. Sci. Instrum.* 43, 832 (1972).
- <sup>20</sup>H. Liskien and A. Paulsen, *Nucl. Data* A11, 569 (1973).
- <sup>21</sup>See Ref. 18.
- <sup>22</sup>S. Hinds, R. Middleton, A. E. Litherland, and D. J. Pullen, *Phys. Rev. Lett.* 6, 113 (1961).
- <sup>23</sup>B. E. F. Macefield, B. Wakefield, and D. H. Wilkinson, *Nucl. Phys.* A131, 250 (1969).
- <sup>24</sup>Y. S. Chen, T. A. Tombrello, and R. W. Kavanagh, *Nucl. Phys.* A146, 136 (1970).
- <sup>25</sup>L. Palfy, J. P. Deutsch, L. Grenacs, J. Lehmann, and M. Steels, *Phys. Rev. Lett.* 34, 212 (1975).
- <sup>26</sup>D. C. Camp and G. L. Meredith, *Nucl. Phys.* A166, 349 (1971).
- <sup>27</sup>I. Dostrovsky, R. Davis, A. M. Poskanzer, and P. L. Reeder, *Phys. Rev.* 139, B1513 (1965).
- <sup>28</sup>D. J. Millener (private communication).
- <sup>29</sup>F. Serduke, 1974 Mass Table, Argonne National Laboratory Report (unpublished).
- <sup>30</sup>J. C. Hardy, J. E. Esterl, R. G. Sextro, and J. Cerny, *Phys. Rev. C* 3, 700 (1971).
- <sup>31</sup>D. H. Wilkinson, *Nucl. Phys.* A179, 289 (1972).
- <sup>32</sup>P. T. Greenland, *J. Phys. G Nucl. Phys.* 1, 1 (1975).